Biomedical Signal Processing and Control 47 (2019) 276–287

Contents lists available at ScienceDirect

Biomedical Signal Processing and Control

journal homepage: www.elsevier.com/locate/bspc

Brain tumor segmentation using neutrosophic expert maximum fuzzy-sure entropy and other approaches

Eser Sert[a,*], Derya Avci[b]

[a] Dept. of Computer Engineering, Engineering and Architecture Faculty, Kahramanmaras Sutcu Imam University, K.Maras, Turkey
[b] Technical Sciences, Department of Computer Technologies, Firat University, 23119, Elazig, Turkey

ARTICLE INFO

Article history:
Received 31 October 2017
Received in revised form 14 July 2018
Accepted 20 August 2018
Available online 5 September 2018

Keywords:
Fuzzy-sure
Neutrosophic set
Support vector machine
Fuzzy C-means
Darwinian particle swarm optimization

ABSTRACT

Glioblastoma is the most aggressive and most common primary brain tumor in adult individuals. Magnetic resonance imagery (MRI) is widely used in the brain tumor diagnosis. This study proposes an approach called neutrosophic set – expert maximum fuzzy-sure entropy (NS-EMFSE), which is a successful edge detection approach, by combining two powerful approaches such as neutrosophic set (NS) and expert maximum fuzzy-sure entropy (EMFSE). Thus, a high performance approach is designed for Glioblastoma, which is the most difficult brain tumor segmentation and edge finding process. The proposed NS-EMFSE approach was designed to detect enhancing part of the tumor in brain MRI image. Using maximum fuzzy entropy and fuzzy c-partition methods, EMFSE determines the necessary threshold value to convert images into binary format. NS has been recently proposed as an efficient approach based on neutrosophy theory, and yields remarkably successful results for indeterminate situations. The proposed algorithm was compared to NS with Otsu thresholding (NS-Otsu), support vector machine (SVM), fuzzy c-means (FCM), Darwinian particle swarm optimization (DPSO). SVM, FCM, DPSO algorithms have been so far used for edge detection and segmentation in various fields. In this study, figure of merid (FOM) and jaccard index (JI) tests were carried out to evaluate the performances of these 5 edge detection approaches on 100 MRI images. These tests indicate which approach yields the best performance in enhancing part detection of the tumor in MRI image. Analysis of variance (ANOVA) was performed on FOM and JI data. As a result, the maximum values of FOM and JI results for the NS-EMFSE are 0.984000, and 0.965000, the mean values are 0.933440 and 0.912000, and the minimum values are 0.699000 and 0.671000, respectively. When these statistical results are compared with the statistical results of other 4 approaches, it is understood that the proposed method yields higher FOM and JI results. In addition, other statistical analysis results proved that the proposed NS-EMFSE performed better than other 4 methods.

1. Introduction

Glioblastoma-type cancers can spread rapidly and are generally likely to lead to a shorter lifespan [1]. In this type of cancer, despite the lack of effective therapies and progress in drug treatments, it is difficult to anticipate the progress of the disease [2].

MRI is widely used to diagnose potential intracerebral problems. It is of vital importance to optimally detect the edges of a tumor or tumors in an MRI image in terms of medical diagnosis and surgical planning. Today, the edges of a tumor/s in an MRI image are manually detected by a radiologist. However, this method is too time-consuming, and might risk overlooking some tumors in the image. As a result, from a medical perspective, it bears utmost importance to automatically detect the edges of a tumor or tumors in an MRI image. It is easier to detect the edges of some brain tumors such as meningiomas, it is more difficult to find brain tumors such as glioma and glioblastoma due to their poorly constrated, low brightness and diffused nature [1]. Therefore, this study focuses on tumor edge detection in MRI images with glioblastomas.

Various approaches have been proposed for tumor edge detection in MRI images such as neural network [1,3], watershed [4], entropy based [5], fuzzy c-means (FCM) algorithm [6], cellular automata [7], stochastic [8], level set [9], support vector machines (SVM) [10], random forests [11], Markov Random Fields [12] and so forth.

In this study, neutrosophic set - expert maximum fuzzy-sure entropy (NS-EMFSE) is proposed as an approach for an automatic tumor edge detection in an MRI image. The first element of the proposed approach, neutrosophic set (NS), is a contemporary approach dealing with the scope, origin and nature of neutralities.

* Corresponding author.
E-mail address: esersert@ksu.edu.tr (E. Sert).

https://doi.org/10.1016/j.bspc.2018.08.025
1746-8094/

Additionally, NS is based on neutrosophy theory, which is a new philosophical branch [13], and is a recent method that successfully resolves indeterminate situations. Thus, it is widely used in various fields such as image processing, filtering, edge detection and segmentation. In the second element of the proposed approach, expert maximum fuzzy-sure entropy (EMFSE), the maximum fuzzy entropy and fuzzy c-partition can automatically detect threshold value at gray level [14]. The method benefits from maximum entropy method, and Sure was used as a type of entropy. This study combines our previous studies on NS [13] and EMFSE [14] to create a more efficient edge detection method. Because NS is a relatively new field of study, its use in the field of biomedical applications [15–18] is limited. In addition, EMFSE has never been used in any biomedical application.

For comparison with NS-EMFSE, NS with Otsu thresholding (NS-Otsu), SVM [19], FCM [20,21] and Darwinian particle swarm optimization (DPSO) [22] algorithms were used. The NS-Otsu approach was obtained using Otsu thresholding [23] instead of the EMFSE used in the NS-EMFSE approach.

An efficient statistical learning method, SVM [19] is widely used in various applications such as segmentation, edge detection and classification. Similarly, FCM [20,21] is an unsupervised technique used in image edge detection, object classification, data mining and machine learning [24]. It is particularly used for edge detection / segmentation in medical images. The particle swarm optimization (PSO) is a powerful machine learning technique. DPSO, which is obtained by adding additional features to the PSO, is an evolutionary algorithm [22]. Ref [22]. provides detailed information on DPSO. The PSO algorithm is frequently used for segmentation and edge detection in brain MRI images [25–27].

The rest of this paper is organized as follows: edge detection approaches are given in Section 2. The approaches for performance evaluation of edge detection are given in Section 3. Experimental results are presented in Section 4. Finally, conclusion is given in Section 5.

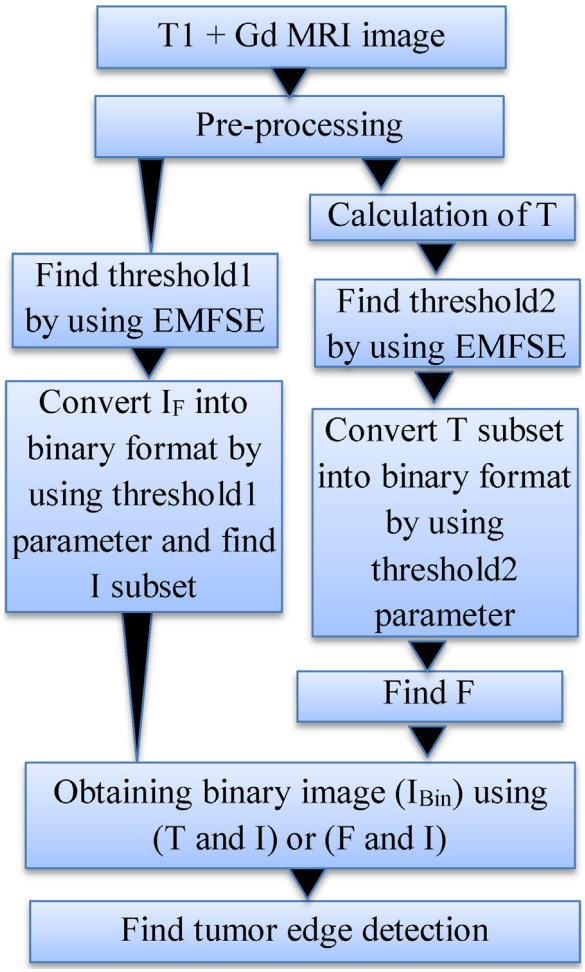

Fig. 1. Converting NS domain of MRI image by using NS-EMFSE.

2. Material and methods

2.1. MRI database

Images in The Cancer Genome Atlas (TCGA) Glioblastoma Multiforme (GBM) collection [28,29] in The Cancer Imaging Archive (TCIA) were used to test the performance of the proposed NS-EMFSE approach. TCGA-GBM collection contains pre-operative MRI images. TCGA-GBM offers open access data for researchers studying brain tumors. Therefore, no ethics committee is required to use the data in this collection. TCGA-GBM offers a rich radiological archive with skull-striped MRI images in NIfTI format in its T1-weighted pre-contrast (T1), T1-weighted post-contrast (T1- gadolinium (Gd), T2, and T2-FLAIR sequences. It is possible to find computer-assisted and manually corrected segmentation ground truth (GT) labels. The proposed NS-EMFSE approach detects enhancing tumor in MRI images. Because T1-Gd sequence is used to collect information about the enhancing and non-enhancing tumor, 100 pieces of 2D slices MRI image (T1-Gd sequence) were used in this study.

2.2. Neutrosophic image

A new approach introduced by Florentine Smarandache, neutrosophy theory is based on a number of disciplines such as neutrosophic logic, neutrosophic probability, neutrosophic set, and neutrosophic statistics [30]. In NS, events are converted to three subsets as True (T), False (F) and Indeterminacy (I). This approach can be used to model indeterminate situations and resolve them successfully [30]. Stock market or weather forecast can be given as examples of indeterminate situations in daily living [30]. Therefore, NS has been widely used in image processing applications. The flow diagram for the conversion of MRI images into NS domain using the proposed NS-EMFSE approach is shown in Fig. 1. This approach pre-processes MRI image at the beginning. Afterwards, EMFSE is used to find I subset in binary format and T and T subsets in binary format as well. This is followed by binary image (I_{Bin}) of the MRI image. Finally, the edges of enhancing tumor are detected.

2.3. Expert maximum fuzzy-sure entropy (EMFSE)

In EMFSE approach, the maximum fuzzy entropy and fuzzy c-partition methods are used to automatically detect threshold method at gray level [14]. In addition to this, Sure entropy was used for maximum entropy as well as c-partition. In this study, EMFSE algorithm is used to convert T, F and I subsets in to binary format [14].

An image has N – gray level ranging from r_0 to r_{j-1}, $W = \{r_0, r_1, \ldots, r_{J-1}\}$. The threshold values obtained from EMFSE correspond to cross points of the fuzzy set as show in Fig. 2. Pixels in this algorithm are divided into two groups as dark and bright groups. For this purpose, two fuzzy sets as dark and bright groups in W are

created, and the equations of this mathematical process are given below [14]:

$$\mu_{\text{dark}}(y) = \begin{cases} 1, & y \le p_1, \\ \dfrac{y - p^3}{p^1 - p^3} & p_1 < y < p_3, \\ 0, & y \ge p_1. \end{cases} \quad (1)$$

$$\mu_{\text{bright}}(y) = \begin{cases} 0, & y \le p_1, \\ \dfrac{y - p^1}{p^3 - p^1} & p_1 < y < p_3, \\ 1, & y \ge p_3 \end{cases} \quad (2)$$

Here, y is an independent variable. Membership functions are p1 and p3 that define the shapes of dark and bright membership functions shown in Fig. 2. EMFSE algorithm was used to determine p_2 parameter which defines the optimal threshold value in this study. The dark membership function of fuzzy set in W variable corresponds to the black pixel group, while the bright membership function of fuzzy set corresponds to the white pixel group.

EMSFE algorithm proposed to detect p_2 parameter is given in Algorithm 1. Algorithm consists of three steps. In the first step, MR image is obtained. In the second step, p_1 and p_3 parameters are determined by using EMFSE [14]. In the last step, p_2 threshold parameter is calculated. More detailed information on the EMFSE algorithm is available in [14].

Algorithm 1. Determing threshold parameter using EMSFE ile threshold

1. Take Input Image (I_{In})
2. I_O histogram is calculated. As a result, $hist_x$ is found, x= 0, . . ., 255.
3. The probability of gray levels is calculated. As a result, Pr (x) = h (x), x = 0, . . ., 255.
4. The exhausted search method is used to calculate $p1_{opt}$ and $p3_{opt}$ parameters. These parameters create a fuzzy 2-partition with a maximum entropy.
5. for p1 = 0: 254
6. for p3 = (p1 + 1) : 255
7. $\mu_{dark}(x)$ and $\mu_{bright}(x)$ membership functions are calculated, x = 0, . . ., 255 for p_1 and p_3
8. The fuzzy probabilities of dark and bright are calculated based on the following equations:

$$Prb\,(dark) = \sum_{x=0}^{255} \mu_{dark}(x)\,\Pr(x),$$

$$Prb\,(bright) = \sum_{x=0}^{255} \mu_{bright}(x)\,\Pr(x),$$

9. Sure Entropy is used to distinguish between dark and bright:

$$|Prb\,(S_i)| \le \varepsilon \Rightarrow H = \sum_{f=0}^{255} \min(Prb\,(S_i)^2\,\varepsilon^2) \quad (\text{for } \varepsilon = 2)$$

$$= \min(\text{Prb (bright)}^2, \varepsilon^2) + \min(\text{Prb (dark)}^2, \varepsilon^2)$$

10. If H > H_{max}
11. H_{max} = H
12. $p1_{opt}$ = p1
13. $p3_{opt}$ = p3
14. end if
15. end for p3
16. end for p1
17. Calculate the Threshold Value that corresponds to the middle point between a_{opt} and c_{opt}:
Threshold value = $p2_{opt}$ = ($p1_{opt}$ + $p3_{opt}$)/2.

2.4. The proposed neutrosophic set expert maximum fuzzy-sure entropy (NS-EMFSE)

NS-EMFSE approach is used to detect the edges of brain tumor/s in an MRI image. This process is detailed in Algorithm 2. It consists of 3 steps:

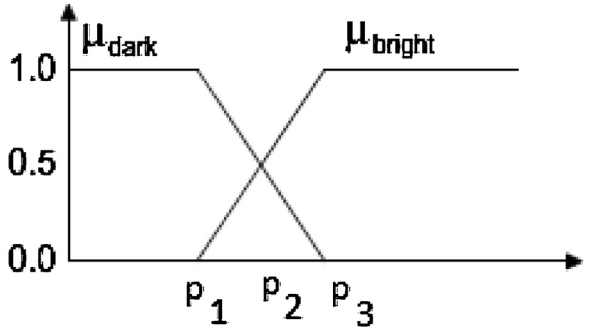

Fig. 2. The membership functions, μ_{dark} and μ_{bright}.

Algorithm 2. Segmentation process using NS-EMFSE

1. img ← Read (T1_Gd MRI Image (NIfTI format file))
% img file sizes=240 x 240 x155 (16 bit integer)
2. mri_file ← img (:,:,slice)
% mri_file sizes = 240 x 240 (16 bit integer)
3. I_G ← Apply Intensity Normalization (mri_file) — Step 1
% I_G sizes = 240 x 240 (8 bit unsigned integer)
4. I_F ← Apply Adaptive Wienering Filter (AWF) to I_G
5. I_{Bin} ← Obtain Binary Format of I_F using NS-EMFSE — Step 2
6. I_{Edge} ← Clean residual pixels in I_{Bin}
7. $I_{Edge\ Detected}$ ← mri_file
8. [Rows Cols] ← Find the number of rows and colums in I_{Edge}
9. for i=1: Rows
10. for j=1: Cols
11. if I_{Edge} (i,j)==1 — Step 3
12. $I_{Edge\ Detected}$ (i, j, 1) ← 255;
13. $I_{Edge\ Detected}$ (i, j, 2) ← 0;
14. $I_{Edge\ Detected}$ (i, j, 3) ← 0;
15. end if
16. end for
17. end for

2.4.1. Pre-processing of MRI image

In this study, MRI files in NIfTI format in TCGA-GBM [28,29] collection were used. A pre-processing is need to process these files using the proposed NS-EMFSE and reach an optimal edge detection performance, which corresponds to Step 1 in Algorithm 2. A 16-bit integer img variable at a dimension of 240 × 240 × 155 was created after MRI Image (T1_Gd sequence) in NIfTI format in Algorithm 2 Line 1 was processed. Because this variable contains 155 pieces of MRI slices (T1_Gd sequence) at a dimension of 240 × 240, the necessary slice was processed using img (:,:,slice) in Line 2 and transferred to mri_file variable. As a result, a 16-bit integer MRI image at a dimension of 240 × 240 was transferred to mri_file variable. Afterwards, intensity normalization was applied to mri_file variable using the process given in Algorithm 3. Thus, 8 bit unsigned integer (8 bit-grayscale format) mri_file variable at a dimension of 240 × 240 was transferred to I_G variable. In this process, MRI image in NIfTI format was converted to a grayscale image at a range of 0–255 to make NS-EMFSE reach a quick and successful edge detection performance.

Algorithm 3. Intensity normalization between 0-255

1. mri_file ← convert to double (mri_file)
2. mri_file ← (mri_file – min (mri_file (:))) / (max (mri_file (:)) – min (mri_file (:)))
3. I_G ← convert to 8 bit unsigned integer (255 * mri_file)

Adaptive Wienering Filter (AWF) [31] was applied to the obtained I_G image in Algorithm 2 in Line 4. AWF is a frequency domain filter whose response varies depending on the statistical characteristics of the image in the filter window [32]. AWF filter is an important filter used to eliminate noise effects in images.

Gaussian filter, mean, average, median, anisotropic diffusion filter (ADF) and AWF filter were used in experimental studies. However, following the pre-processing with these filters, the results of Jaccard Index (JI) and Figure of Merid (FOM) analysis on NS-EMFSE

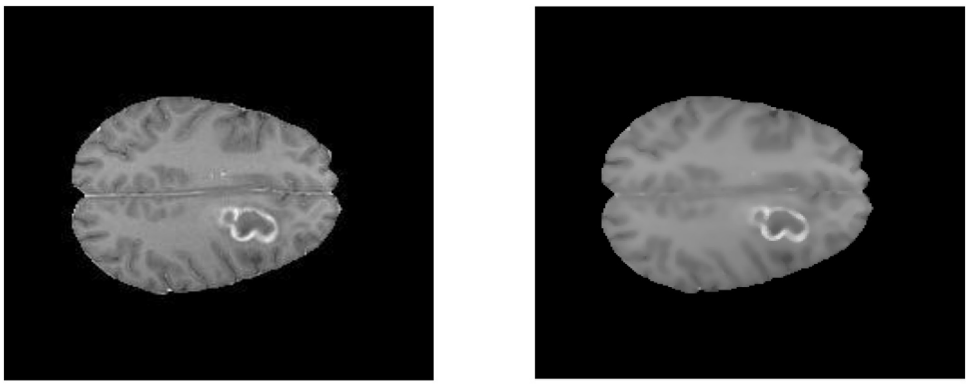

Fig. 3. MRI Image and I_F: (a) MRI image; (b) Filtered image (I_F).

tumor edge finding results were analyzed, and the most successful edge finding performance was obtained via AWF filter. $Image_{Filtered}$ (I_F) was obtained after AWF was applied to the MRI image. MRI Image and I_F are shown in Fig. 3.

2.4.2. Obtaining binary image using NS-EMFSE

In the Step 2 in Algorithm 2, I_{Bin}, which is the binary image of pre-processed MRI image (I_F), is obtained via NS-EMFSE. Therefore, as shown in the flow diagram in Fig. 1, T, I and F subsets are calculated to find Binary Image (I_{Bin}).

(a) Obtaining T and F Subsets:

In this study, the method proposed by Zhang et al. [33] and the modified Norm Entropy in S-Function [13] are used in order to obtain T subset. The algorithmic process used to obtain T and F subsets and their binary format (T_Binary and F_Binary) is given in Algorithm 4. At the beginning of this process, g is applied to S-Function. Thanks to S-Function, as explained below, the brightness level of signal gray level is represented [13,33,34]:

$$T(i,j) = \text{S-function}(g; prt_1, prt_2, prt_3) \tag{3}$$

The intensity value of I_F at (i, j) coordinate is g. Input parameters that define the shape of S-Function are prt_1, prt_2, prt_3. The intensity values that correspond to the leftmost and rightmost peak values of histogram of I_F are prt_1 and prt_3, respectively. The maximum norm entropy principle given below is used to calculate prt_2 [35]:

$$H(I_F) = \frac{1}{MxN}\sum_{j}^{N}\sum_{i}^{M}\text{Norm Entropy(T)} \tag{4}$$

where M and N to rows and columns. H, which corresponds to Entropy value, is directly proportionate to the amount of information [35,36]. The most optimal prt_2 (prt_{2opt}) value is obtained by trying all values from prt_3 -1 to prt_1 +1 [36]. When $prt_{2\ opt}$ value is obtained, maximum H can also be found. The norm entropy mathematically defined in Eq. (5) was preferred because of its superiority to other types of entropy in terms of segmentation performance. More information about prt_1, prt_2, prt_3 parameters and T subset can be found in ref. [13,33].

$$\text{Norm}\quad \text{Entropy}(T) = \left|T_{(i,j)}\right|^p \tag{5}$$

where $1 \le p < 2$. After T subset is found, threshold parameter of T subset is obtained by using EMFSE algorithm [14], and it is named threshold2. In the next step, this parameter is used to convert T subset into binary format, and the skull image is removed from this binary image thanks to morphology and other similar methods, thus obtaining the brain image. The resulting image is named T_Binary. Finally, F subset is calculated thanks to the following equation:

$$F\_Binary = 1 - T\_Binary \tag{6}$$

Algorithm 4. Obtaining T_Binary and F_Binary subsets

1. $H_{max} \leftarrow$ - Infinity
2. Find prt_2, prt_1 [33]
3. for $sp_{2op\,t} \leftarrow$ from $prt_3 - 1$ to $prt_1 + 1$
4. T ← S-Function (g; prt_1, ptr_2, prt_3)
5. $H = \frac{1}{MxN}\sum_{j}^{N}\sum_{i}^{M}\text{Norm Entropy(T)}$
6. if $H > H_{max}$
7. $H_{max} \leftarrow H$
8. $prt_{2opt} \leftarrow prt_2$
9. end
10. end for
11. $prt_2 \leftarrow prt_{2opt}$
12. T ← S Function (d_{ij}; prt_1, prt_2, prt_3)
13. threshold2 ← EMFSE (T)
14. T_Intermediate ← Convert to Binary (T, threshold1)
15. T_Binary ← Remove the skull image in T_Intermediate and clean residual pixels
16. F_Binary ← 1 – T_Binary

T and F subsets and T_Binary and F_Binary images obtained as a result of this process are given in Fig. 4. As shown in Fig. 4.c and Fig. 4.d, the brain is kept under T subset and brain background under F subset, respectively.

(b) Obtaining I Subset

In the first step, in order to calculate I, I_F is processed by EMFSE algorithm to find threshold parameter, which is named threshold1. I_F is converted to binary image using the threshold1 parameter, and then edge image of the binary image is obtained. The obtained edge image is called Homogenity_Binary (H_Binary) image. H_Binary image is related to the local information, and the values of related pixels of H_Binary increase during object and background transitions [30]. After H image is found, Eq. (7) is used to calculate I_Binary subset. In this subset, indeterminate situations such as skull, color transition of tumors and noise can be detected. The resulting images are shown in Fig. 5. MRI images (T1-Gd sequence) in NIfTI format in TCGA-GBM collection [28,29] were prepared as skull-stripped. However, in order to improve the performance of the proposed

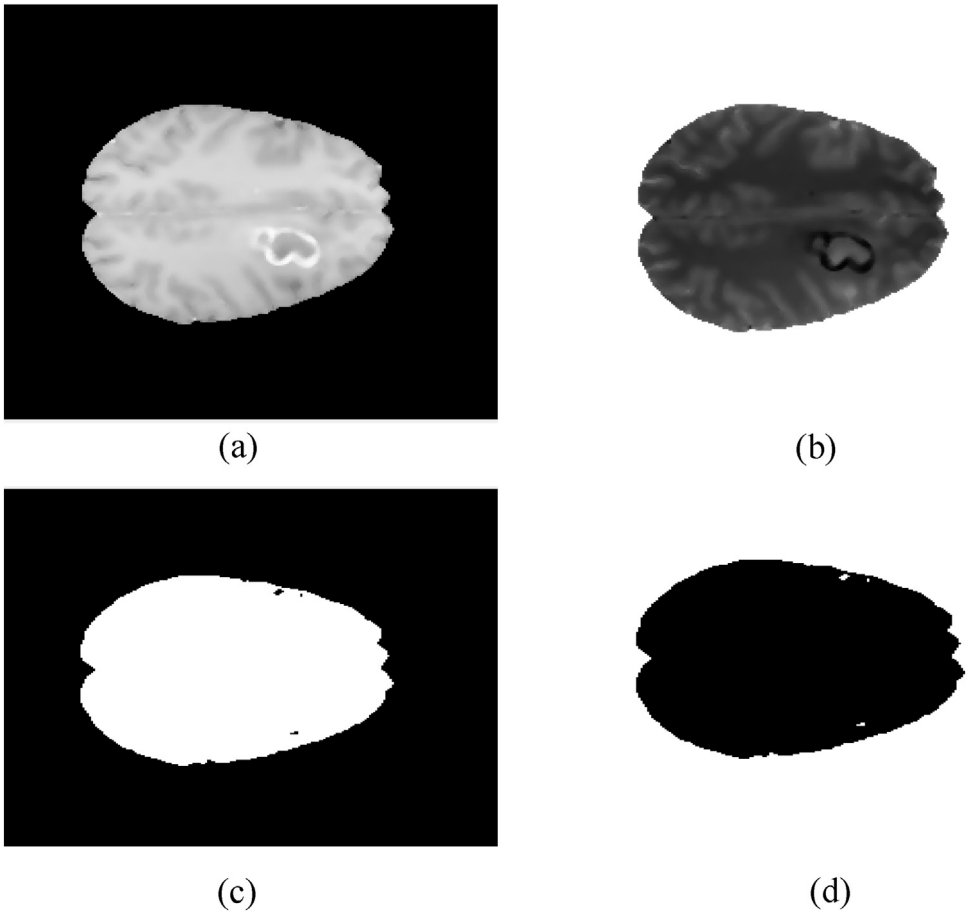

Fig. 4. Resulting images: (a) T Subset Image; (b) F subset image; c) T_Binary subset image; (d) F_Binary subset image.

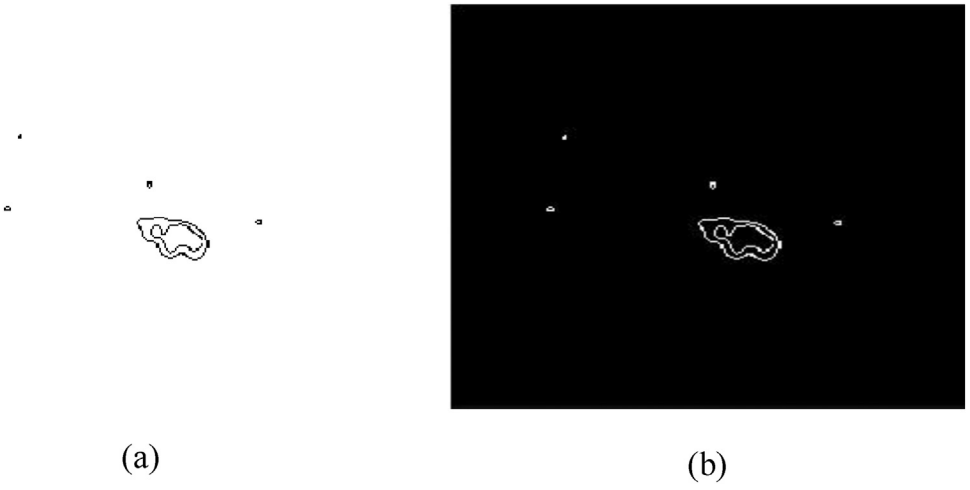

Fig. 5. Resulting images: (a) H_Binary Image; (b) I_Binary subset image.

NS-EMFSE approach, possible skulls in MRI images were detected in I_Binary subset.

$$\text{I\_Binary} = 1 - \text{H\_Binary} \tag{7}$$

(c) Obtaining Binary image (I_{Bin})

I_{Bin} is an image obtained by using T_Binary and I_Binary subsets, or F_Binary and I_Binary subsets. Accordingly, I_{Bin} is calculated in accordance with either formula Eqs. (8) and (9). The I_{Bin} obtained at the end of this process is given in Fig. 6. When an image containing skull was used, skull images were omitted from I_{Bin} image using Eqs. (8) and (9) because skull and tumors would be found in I subset and brain T subset. As a result, I_{Bin} contains tumor and very small residual images.

$$I_{Bin} = \text{T\_Binary} * \text{I\_Binary} \tag{8}$$

$$I_{Bin} = (\text{F\_Binary})' * \text{I\_Binary} \tag{9}$$

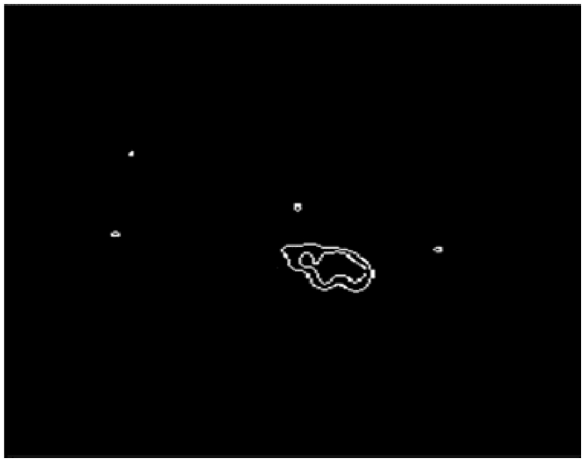

Fig. 6. I_{Bin}.

2.4.3. Tumor edge detection

In the Step 3 in Algorithm 2, tumor edge detection process is performed. Since I_{Bin} image contains very small residual images close to the tumor, these residual images are deleted by morphological methods in line 6 in Algorithm 2, and the resulting image is saved with the name I_{Edge}. MRI Image is transferred to the $I_{Edge\ Detected}$ variable in line 7. Because tumor edges only appear on I_{Edge}, the algorithmic process in line-8 and line-17 is carried out in order for these edges to appear in red on the MR image named as $I_{Edge\ Detected}$. I_{Edge} and $I_{Edge\ Detected}$ images obtained end of this step are given in Fig. 7(a) and (b).

2.5. NS with Otsu thresholding

As discussed in Section 2.4.2, the EMFSE approach is used to determine the threshold parameter of the T and I subsets in the proposed NS-EMFSE. In order to analyze the performance of the proposed approach, NS-Otsu was designed using Otsu's thresholding [23] method instead of the EMFSE approach used in NS-EMFSE. Otsu's method is one of the most widely used thresholding methods and performs on a clustering basis [23]. The method fails to calculate the threshold value when the histogram of the used image is close to unimodal or unimodal [37]. The processing results of MRI image via the NS-Otsu approach in Fig. 8(**a**) are shown in Fig. 8(**b**–**g**).

3. Evaluation methods for edge detection performance

JI [38] and FOM [39], the most popular tests for the evaluation of edge detection performance, were used in this study. JI is a statistical measurement method that yields the similarity between the image I_{Edge}, which is obtained using the edge detection approach, and (I_{GT}), which is the ground truth image that expresses the manual edge detection. JI is calculated as follows [38]:

$$JI = \frac{|I_{GT|} \cap |\text{Iedge}|}{|I_{GT|} \cup |\text{Iedge}|} \tag{10}$$

On the other hand, FOM [39], which was proposed by Pratt, is one of the most successful methods for the evaluation of edge detection performance. FOM is calculated as follows:

$$\text{FOM} = \frac{1}{\max(N_{DT}, N_{AC})} \sum_{i=1}^{N_{DT}} \frac{1}{1 + dm^2(i)} \tag{11}$$

where N_{DT} *and* N_{AC} corresspond to the number of points detected by edge detection approach and actual edge points, respectively. The distance to the i^{th} actual edge point is m (i). The scaling constant is d. Although FOM value varies between 0 and 1, the segmentation performance is higher if this value converges to 1.

4. Experimental results

The present study benefits from MRI images (T1-Gd sequence) in TCGA-GBM collection [28,29] to conduct experimental studies. In this respect, NS – EMFSE, NS-Otsu, SVM, FCM, DPSO algorithms were used to detect the edges of brain tumors in 100 different MRI images, and the results of the first 7 tests are shown in Figs. 9 and 10. These images contain MRI images (T1-Gd sequence) used in the first 7 tests, GT images including enhancing tumor of these images, edge detected - ground truth (ED-GT) images and edge detection results. Because the proposed NS-EMFSE approach was designed to detect enhancing tumor, GT obtained from TCGA-GBM was re-arranged to leave enhancing part alone. ED-GT images shown in Fig. 9 and **10** were obtained by detecting the edges of GT image using sobel operator. NS-EMFSE and NS-Otsu edge detections results are shown in Fig. 9, and SVM, FCM and DPSO edge detection results are shown in Fig. 10. As the related figures also demonstrate, the proposed algorithm displayed a much more successful edge detection performance.

FOM and JI tests were performed to find out the performance of the 5 edge detection approach. These tests mainly aim to indicate which approach yields the best performance in enhancing part detection of the tumor in MRI image (T1-Gd sequence). Therefore, ED-GT image of the tested MRI image and edge detection result of

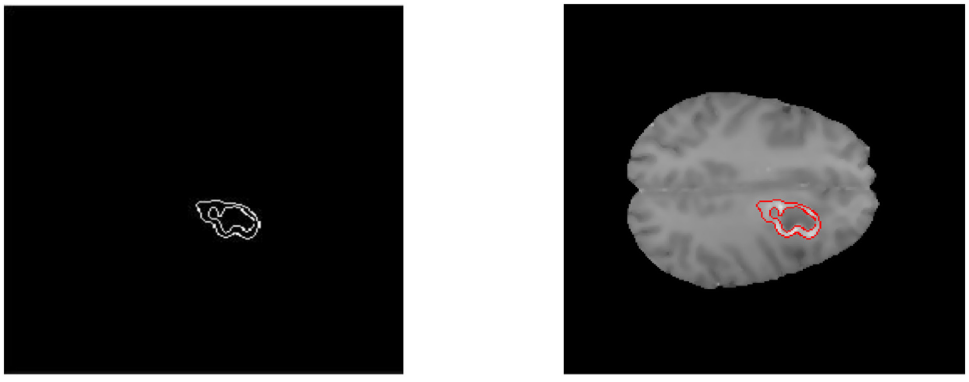

Fig. 7. Analysis results: (a) $I_{Edge;}$ (b) $I_{Edge\ Detected}$.

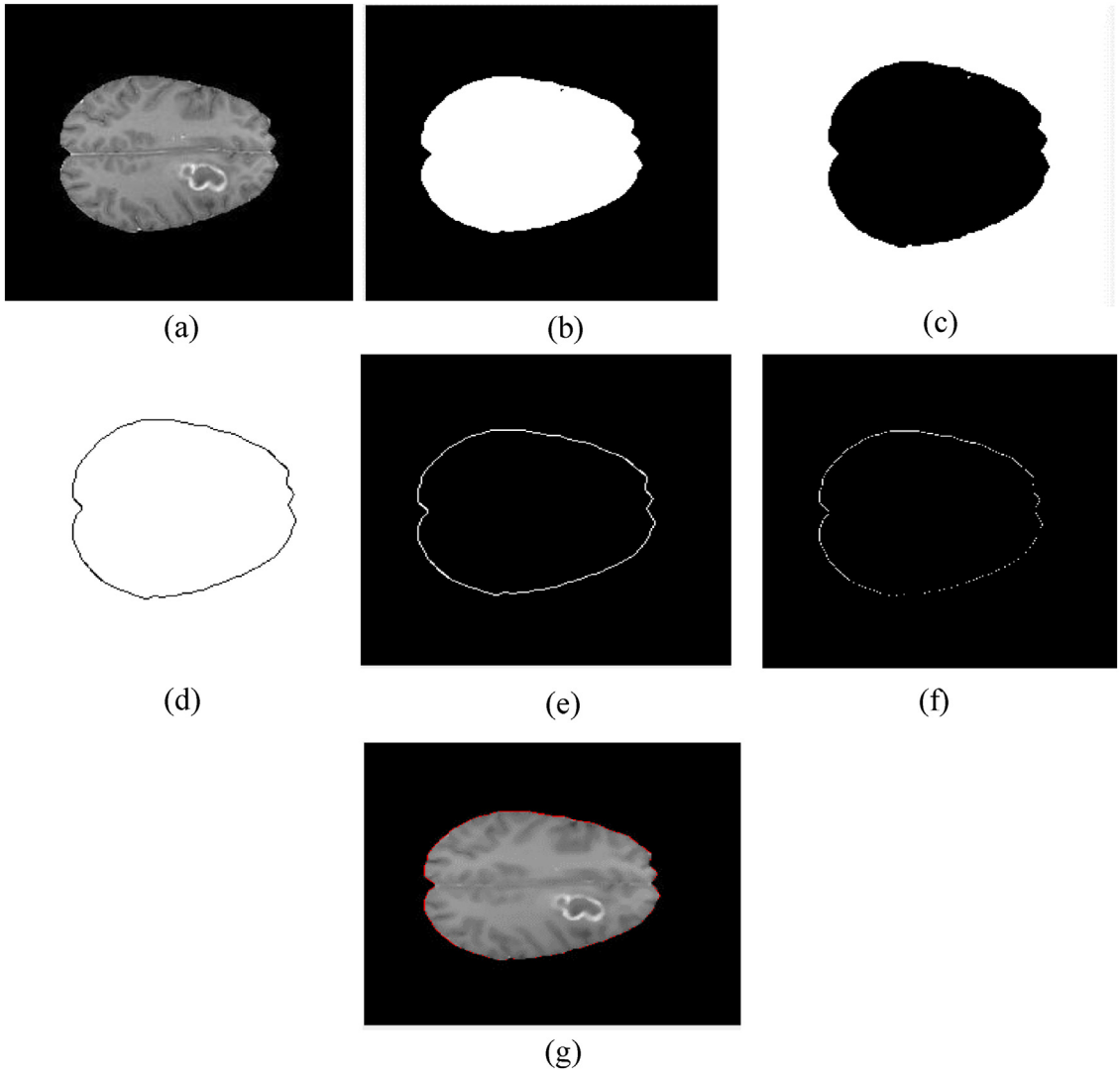

Fig. 8. MRI Image and resulting images: (a) MRI image; (b) T_Binary subset image; (c) F_Binary subset image; (d) H_Binary Image; (e) I_Binary subset image; (f) $I_{Edge,}$ (g) $I_{Edge\ Detected}$.

Table 1
FOM statistics with ANOVA.

FOM Score Edge Detection Method	N	Mean	Std. Deviation	Std. Error	95% Confidence Interval for Mean Lower Bound	Upper Bound	Minimum	Maximum
NS-EMFSE	100	0.933440	0.041233	0.004123	0.925259	0.941621	0.699000	0.984000
NS-Otsu	100	0.059510	0.055841	0.005584	0.048430	0.070590	0.000000	0.274000
SVM	100	0.051220	0.057941	0.005794	0.039723	0.062717	0.000000	0.379000
FCM	100	0.124100	0.090656	0.009066	0.106112	0.142088	0.019000	0.394000
DPSO	100	0.369700	0.131855	0.013185	0.343537	0.395863	0.040000	0.794000
Total	500	0.307594	0.343834	0.015377	0.277383	0.337805	0.000000	0.984000

the edge detection approach were compared in FOM and JI tests, and edge detection performances of 5 edge detection approaches for 100 MRI images produced 500 pieces of FOM and 500 pieces of JI test results. Graphic illustration of these FOM and JI results are shown in Figs. 11 and 12, respectively. Additionally, these FOM and JI results were statistically analyzed, and the results are given in Table 1. Because the statistical results of NS – EMFSE yielded much more successful results compared to other approaches, it is evident that the proposed method detects the edges of brain tumors in the most efficient way.

Analysis of variance (ANOVA) was applied to 500 FOMs and 500 JI results, including 100 FOMs and 100 JIs obtained from each edge detection approach:

1) At first, the statistical analysis results of FOM analysis results obtained via 5 edge detection approaches are given in Table 1. From the statistical results, it can inferred from these results that for the proposed NS-EMFSE method, mean, 95% confidence interval for mean, minimum and maximum values are higher and std. deviation is lower compared to other methods. There-

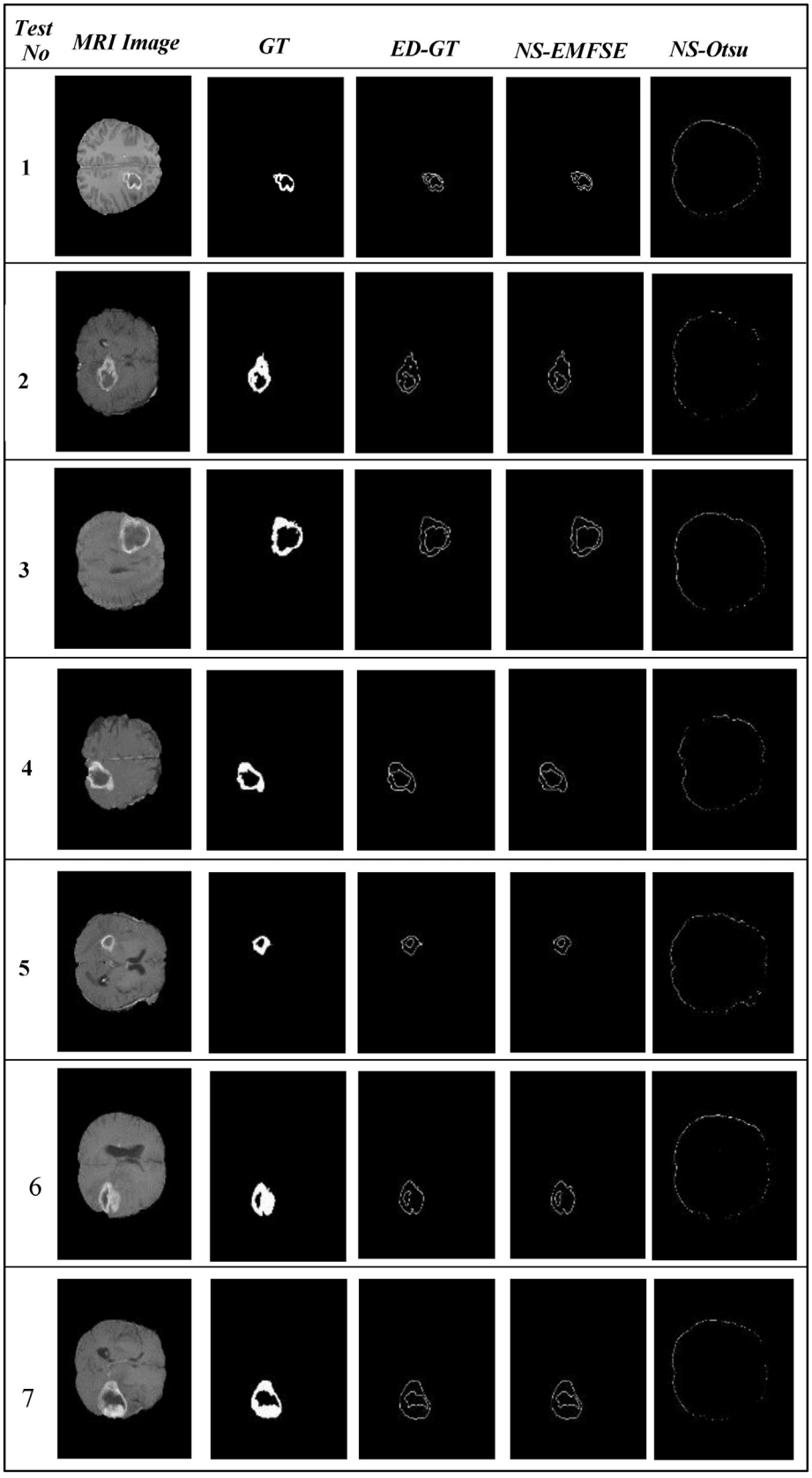

Fig. 9. Test results.

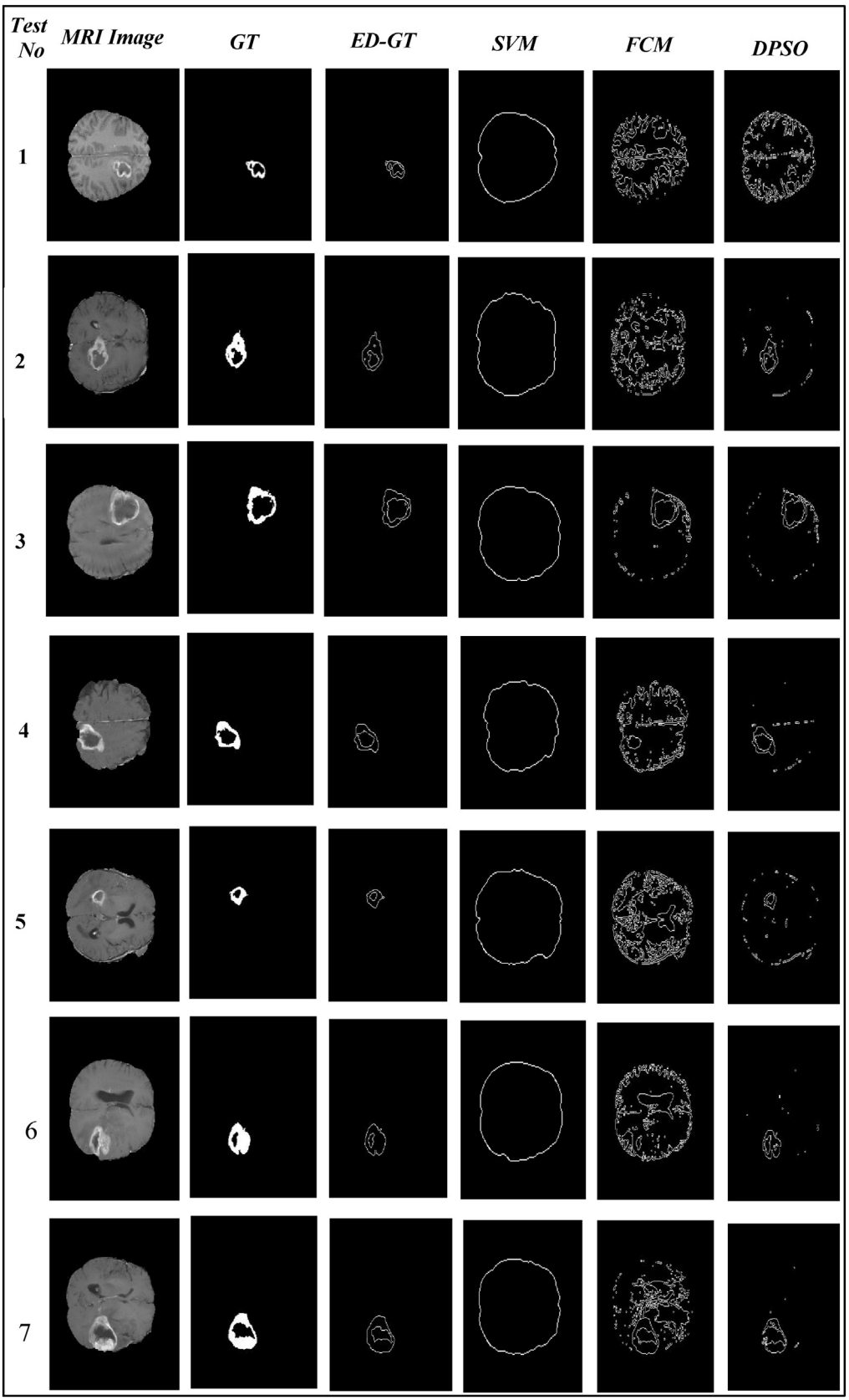

Fig. 10. Test results.

Table 2
Significance report of FOM with ANOVA.

FOM Score					
	Sum of Squares	df	Mean Square	F	Sig.
Between Groups	55.648372	4	13.912093	2059.244533	0.000000
Within Groups	3.344181	495	0.006756		
Total	58.992553	499			

fore, the statistically proposed NS-EMFSE method displayed superior edge detection performance compared to others.

2) When Table 2 is analyzed, it can be observed that the results of FOM analysis obtained via 5 different edge detection approaches differ statistically ($F(4495) = 2059.245$; $p = 0.000 < 0.05$). Post Hoc analysis, which is a multiple comparison test, was performed to determine statistical differences among groups, and the analysis results are given in Table 3. Std. Error of the difference between the two means of Edge Detection Method 1 and 2 in the table is calculated based on the following formula:

$$\text{Std.Error}(\text{Edge Detection Method 1} - \text{Edge Detection Method 2}) = \sqrt{\text{MS} \cdot \left(\frac{1}{N_1} + \frac{1}{N_2}\right)} \quad (12)$$

Here, the1 MS value corresponds to the Mean Square value corresponding to the Within Groups given in Ŝignificance report of FOM with ANOVAẗable. N_1 and N_2 values correspond to the number of tests in Edge Detection Method 1 and Edge Detection Method 2, respectively. Since the number of the FOM tests performed for all the edge detection methods in this study is 100, N_1 and N_2 are 100. To ensure standardization in the presentation of the test results, the number of decimal digits following the comma is set to 6 from Tables 1–6. As can be seen from Table 2, MS is 0.006756 for all edge detection methods. Therefore, all the Std. Error values in Table 3 were obtained as 0.011624 via using of Eq. (12). When Table 3 is analyzed, it is evident that NS-EMFSE is the approach with the highest Mean Difference (I–J), which demonstrates the differences of average FOM values between the two methods, and SVM is the approach with the lowest Mean Difference (I–J). Based on these statistical results, it can be concluded that the most successful edge detection approach is NS-EMFSE while the most unsuccessful approach is SVM.

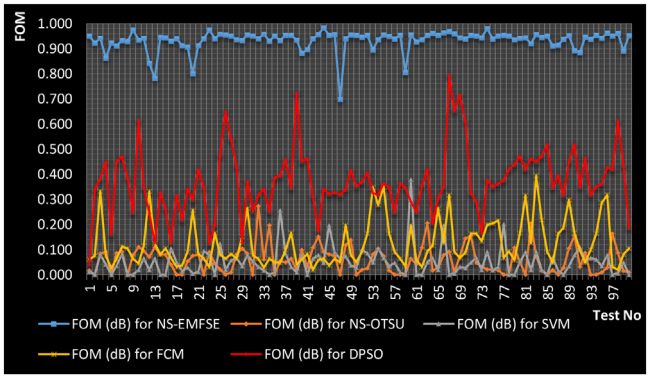

Fig. 11. FOM result graph.

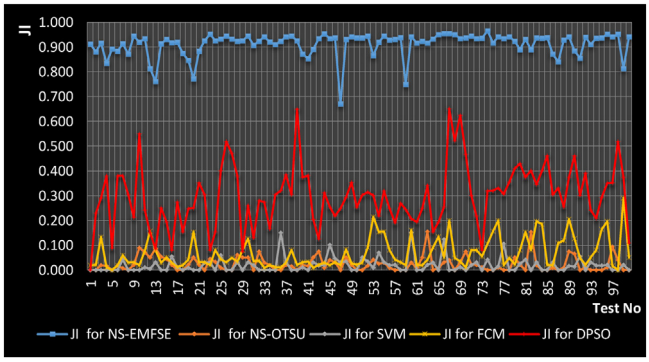

Fig. 12. JI result graph.

3) Statistical analysis performed for FOM results were also performed for JI results, and the results are given in Tables 4–6. All the Std. Error values in Table 6 were obtained as 0.009681 via

Table 3
Post Hoc comparison of FOM.

FOM Score						
Multiple Comparisons. Test: Scheffe						
(I) Edge Detection Method	(J) Edge Detection Method	Mean Difference (I-J)	Std. Error	Sig.	95% Confidence Interval	
					Lower Bound	Upper Bound
NS-EMFSE	NS-Otsu	0.873930[a]	0.011624	0.000	0.83799	0.90987
	SVM	0.882220[a]	0.011624	0.000	0.84628	0.91816
	FCM	0.809340[a]	0.011624	0.000	0.77340	0.84528
	DPSO	0.563740[a]	0.011624	0.000	0.52780	0.59968
NS-Otsu	NS-EMFSE	−0.873930[a]	0.011624	0.000	−0.90987	−0.83799
	SVM	0.008290	0.011624	0.973	−0.02765	0.04423
	FCM	−0.064590[a]	0.011624	0.000	−0.10053	−0.02865
	DPSO	−0.310190[a]	0.011624	0.000	−0.34613	−0.27425
SVM	NS-EMFSE	−0.882220[a]	0.011624	0.000	−0.91816	−0.84628
	NS-Otsu	−0.008290	0.011624	0.973	−0.04423	0.02765
	FCM	−0.072880[a]	0.011624	0.000	−0.10882	−0.03694
	DPSO	−0.318480[a]	0.011624	0.000	−0.35442	−0.28254
FCM	NS-EMFSE	−0.809340[a]	0.011624	0.000	−0.84528	−0.77340
	NS-Otsu	0.064590[a]	0.011624	0.000	0.02865	0.10053
	SVM	0.072880[a]	0.011624	0.000	0.03694	0.10882
	DPSO	−0.245600[a]	0.011624	0.000	−0.28154	−0.20966
DPSO	NS-EMFSE	−0.563740[a]	0.011624	0.000	−0.59968	−0.52780
	NS-Otsu	0.310190[a]	0.011624	0.000	0.27425	0.34613
	SVM	0.318480[a]	0.011624	0.000	0.28254	0.35442
	FCM	0.245600[a]	0.011624	0.000	0.20966	0.28154

[a] The mean difference is significant at the 0.05 level.

Table 4
JI statistics with ANOVA.

JI Score Edge Detection Method	N	Mean	Std. Deviation	Std. Error	95% Confidence Interval for Mean Lower Bound	Upper Bound	Minimum	Maximum
NS-EMFSE	100	0.912000	0.048043	0.004804	0.902467	0.921533	0.671000	0.965000
NS-Otsu	100	0.024900	0.030973	0.003097	0.018754	0.031046	0.000000	0.155000
SVM	100	0.019420	0.030231	0.003023	0.013421	0.025419	0.000000	0.151000
FCM	100	0.067040	0.061184	0.006118	0.054900	0.079180	0.000000	0.290000
DPSO	100	0.297470	0.124536	0.012454	0.272759	0.322181	0.000000	0.651000
Total	500	0.264166	0.346759	0.015508	0.233698	0.294634	0.000000	0.965000

Table 5
Significance report of JI with ANOVA.

JI Score					
	Sum of Squares	df	Mean Square	F	Sig.
Between Groups	57.680553	4	14.420138	3076.747525	0.000000
Within Groups	2.319972	495	0.004687		
Total	60.000525	499			

Table 6
Post Hoc comparison of JI.

FOM Score						
Multiple Comparisons. Test: Scheffe						
(I) Edge Detection Method	(J) Edge Detection Method	Mean Difference (I-J)	Std. Error	Sig.	95% Confidence Interval	
					Lower Bound	Upper Bound
NS-EMFSE	NS-Otsu	0.887100[a]	0.009681	0.000000	0.857165	0.917035
	SVM	0.892580[a]	0.009681	0.000000	0.862645	0.922515
	FCM	0.844960[a]	0.009681	0.000000	0.815025	0.874895
	DPSO	0.614530[a]	0.009681	0.000000	0.584595	0.644465
NS-Otsu	NS-EMFSE	−0.887100[a]	0.009681	0.000000	−0.917035	−0.857165
	SVM	0.005480	0.009681	0.988424	−0.024455	0.035415
	FCM	−0.042140[a]	0.009681	0.000930	−0.072075	−0.012205
	DPSO	−0.272570[a]	0.009681	0.000000	−0.302505	−0.242635
SVM	NS-EMFSE	−0.892580[a]	0.009681	0.000000	−0.922515	−0.862645
	NS-Otsu	−0.005480	0.009681	0.988424	−0.035415	0.024455
	FCM	−0.047620[a]	0.009681	0.000093	−0.077555	−0.017685
	DPSO	−0.278050[a]	0.009681	0.000000	−0.307985	−0.248115
FCM	NS-EMFSE	−0.844960[a]	0.009681	0.000000	−0.874895	−0.815025
	NS-Otsu	0.042140[a]	0.009681	0.000930	0.012205	0.072075
	SVM	0.047620[a]	0.009681	0.000093	0.017685	0.077555
	DPSO	−0.230430[a]	0.009681	0.000000	−0.260365	−0.200495
DPSO	NS-EMFSE	−0.614530[a]	0.009681	0.000000	−0.644465	−0.584595
	NS-Otsu	0.272570[a]	0.009681	0.000000	0.242635	0.302505
	SVM	0.278050[a]	0.009681	0.000000	0.248115	0.307985
	FCM	0.230430[a]	0.009681	0.000000	0.200495	0.260365

[a] The mean difference is significant at the 0.05 level.

using of Eq. (12). The statistical results indicate that the JI results obtained via NS-EMSE approach are remarkably higher compared to the other methods, while the results of SVM approach are lower compared to other methods. Therefore, it can be argued that NS-EMFSE offers the most successful edge detection performance, while SVM displays the most unsuccessful edge detection performance.

5. Conclusion

In this study, NS-EMFSE approach was proposed to detect the edges of brain tumors in an MRI image. NS-Otsu, SVM, FCM and DPSO approaches were used to compare the proposed method with other methods. When the proposed method and other 4 methods were applied to the MRI images with 100 different brain tumors, the edge detection results obtained from these images were statistically analyzed. As a result, arithmetic means of NS – EMFSE for FOM and JI test results were calculated as 0.933440 and 0.912000, respectively. These results suggest that NS – EMFSE is more efficient compared to the arithmetic means of other four methods for FOM and JI results, indicating its remarkable success in edge detection. In addition, other statistical analysis results proved that proposed NS-EMFSE method displayed superior edge detection performance compared to others.

References

[1] M. Havaei, A. Davy, D. Warde-Farley, A. Biard, A. Courville, Y. Bengio, C. Pal, P.-M. Jodoin, H. Larochelle, Brain tumor segmentation with deep neural networks, Med. Image Anal. 35 (2017) 18–31.
[2] R.-Y. Bai, V. Staedtke, G.J. Riggins, Molecular targeting of glioblastoma: drug discovery and therapies, Trends Mol. Med. 17 (2011) 301–312.
[3] A.A. Abdullah, B.S. Chize, Z. Zakaria, Design of cellular neural network (CNN) simulator based on matlab for brain tumor detection, J. Med. Imaging Health Inform. 2 (2012) 296–306.
[4] M.M.J. Letteboer, W.J. Niessen, P.W.A. Willems, E.B. Dam, M.A. Viergever, Interactive multi-scale watershed segmentation of tumors in MR brain images, in: Proceedings of Interactive Medical Image Visualization And Analysis, 2001, pp. 11–16.

[5] V. Rajinikanth, S.C. Satapathy, S.L. Fernandes, S. Nachiappan, Entropy based segmentation of tumor from brain MR images – a study with teaching learning based optimization, Pattern Recognit. Lett. 94 (2017) 87–95.
[6] S.V.A. Kumar, B.S. Harish, V.N.M. Aradhya, A picture fuzzy clustering approach for brain tumor segmentation, Second International Conference on Cognitive Computing and Information Processing (2016) 1–6.
[7] C. Sompong, S. Wongthanavasu, An efficient brain tumor segmentation based on cellular automata and improved tumor-cut algorithm, Expert Syst. Appl. 72 (2017) 231–244.
[8] L. Farhi, A. Yusuf, R.H. Raza, Adaptive stochastic segmentation via energy-convergence for brain tumor in MR images, J. Vis. Commun. Image R. 46 (2017) 303–311.
[9] K. Thapaliya, J.-Y. Pyun, C.-S. Park, G.-R. Kwon, Level set method with automatic selective local statistics for brain tumor segmentation in MR images, Comput. Med. Imaging Graph. 37 (2013) 522–537.
[10] J. Zhang, K. Ma, M. Er, V. Chong, Tumor segmentation from magnetic resonance imaging by learning via one-class support vector machine, in: Wokshop on Advanced Image Technology, 2004, pp. 207–211.
[11] N. Tustison, K.L. Shrinidhi, M. Wintermark, C.R. Durst, B.M. Kandel, J.C. Gee, M.C. Grossman, B.B. Avants, Optimal symmetric multimodal templates and concatenated random forests for supervised brain tumor segmentation (simplified) with ANTsr, Neuroinformatics 13 (2015) 209–225.
[12] K. Held, E. Kops, B. Krause, W. Wells, R. Kikinis, Markov random field segmentation of brain MR images, IEEE Trans. Med. Imaging 16 (1997) 878–886.
[13] E. Sert, A new modified neutrosophic set segmentation approach, Comput. Electr. Eng. 65 (2018) 576–592.
[14] E. Avci, D. Avci, An expert system based on fuzzy entropy for automatic threshold selection in image processing, Expert Syst. Appl. 36 (2009) 3077–3085.
[15] S. Dhar, M.K. Kundu, Accurate segmentation of complex document image using digital shearlet transform with neutrosophic set as uncertainty handling tool, Appl. Soft Comput. 61 (2017) 412–426.
[16] Y. Guo, G.-Q. Du, J.-Y. Xue, R. Xia, Y.-H. Wang, A novel myocardium segmentation approach based on neutrosophic active contour model, Comput. Methods Programs Biomed. 142 (2017) 109–116.
[17] M. Lotfollahi, M. Gity, J. Yong Ye, A. Mahlooji Far, Segmentation of breast ultrasound images based on active contours using neutrosophic theory, J. Med. Ultrasonics 45 (2) (2017) 205–212.
[18] D. Koundal, S. Gupta, S. Sing, Automated delineation of thyroid nodules in ultrasound images using spatial neutrosophic clustering and level set, Appl. Soft Comput. 40 (2016) 86–97.
[19] C. Cortes, V. Vapnik, Support vector networks, Mach. Learn. 20 (3) (1995) 273–297.
[20] R. Suganya, R. Shanthi, Fuzzy c- means algorithm- a review, Int. J. Sci. Res. Publ. 2 (11) (2012) 1–3.
[21] J.C. Bezdek, R. Ehrlich, W. Full, FCM: the fuzzy c-means clustering algorithm, Comput. Geosci. 10 (1984) 191–203.
[22] M.S. Couceiro, R.P. Rocha, N.M.F. Ferreira, J.A.T. Machado, Introducing the fractional-order darwinian PSO, signal, Image and Video Processing 6 (2012) 343–350.
[23] N. Otsu, A threshold selection method from gray-level histograms, IEEE Trans. Syst. Man Cybern. 9 (1979) 62–66.
[24] M.K. Alsmadi, A hybrid fuzzy c-means and neutrosophic for jaw lesions segmentation, Ain Shams Engineering Journal (2016), https://doi.org/10.1016/j.asej.2016.03.016.
[25] F. Hamdaoui, A. Ladgham, A. Sakly, A. Mtibaa, A new images segmentation method based on modified particle swarm optimization algorithm, Int. J. Imaging Syst. Technol. 23 (2013) 265–271.
[26] Salim Lahmiri, Glioma detection based on multi-fractal features of segmented brain MRI by particle swarm optimization techniques, Biomed. Signal Process. Control 31 (2017) 148–155.
[27] D.R. Nayakagliobl, R. Dasha, B. Majhi, Discrete ripplet-II transform and modified PSO based improved evolutionary extreme learning machine for pathological brain detection, Neurocomputing 282 (2018) 232–247.
[28] S. Bakas, H. Akbari, A. Sotiras, M. Bilello, M. Rozycki, J. Kirby, J. Freymann, K. Farahani, C. Davatzikos, Segmentation labels and radiomic features for the pre-operative scans of the TCGA-GBM collection, Cancer Imaging Arch. (2017), http://dx.doi.org/10.7937/K9/TCIA.2017.KLXWJJ1Q.
[29] S. Bakas, H. Akbari, A. Sotiras, M. Bilello, M. Rozycki, J.S. Kirby, J.B. Freymann, K. Farahani, C. Davatzikos, Advancing the cancer genome atlas glioma MRI collections with expert segmentation labels and radiomic features, Nat. Sci. Data 4 (2017) 170117.
[30] F. Smarandache, A Unifying Field In Logics Neutrosophic Logic, Neutrosophy, Neutrosophic Set, Neutrosophic Probability, American Research Press, 2003.
[31] R.C. Hardie, A fast image super-resolution algorithm using an adaptive Wiener filter Dec, IEEE Trans. Image Process. 16 (2007) 2953–2964.
[32] S.S. Al-amri, N.V. Kalyankar, S.D. Khamitkar, A comparative study of removal noise from remote sensing image, IJCSI Int. J. Comput. Sci. Issues 7 (2010), 32-26.
[33] M. Zhang, L. Zhang, H.D. Cheng, A neutrosophic approach to image segmentation based on watershed method, Signal Processing 90 (2010) 1510–1517.
[34] H.D. Cheng, J.R. Chen, Automatically determine the membership function based on the maximum entropy principle, Inf. Sci. 96 (1997) 163–182.
[35] H.D. Cheng, J. Wang, X. Shi, Microcalcication detection using fuzzy logic and scale space approaches, Pattern Recognit. 37 (2004) 363–375.
[36] H.D. Cheng, H. Xu, A novel fuzzy logic approach to contrast enhancement, Pattern Recognit. 33 (2000) 809–919.
[37] X.-C. Yuana, L.-S. Wua, Q. Peng, An improved Otsu method using the weighted object variance for defect detection, Appl. Surf. Sci. 349 (2015) 472–484.
[38] C.-Y. Yua, W.-S. Zhang, Y.-Y. Yub, Y. Li, A novel active contour model for image segmentation using distance regularization term, Comput. Math. With Appl. 65 (2013) 1746–1759.
[39] W.K. Pratt, Digital Image Processing, John Wiley & Sons, 1978.